ARL-TR-8181 ● Oct 2017

US Army Research Laboratory

Detection of Explosives on Surfaces Using UV Raman Spectroscopy: Effect of Substrate Color

by Cole Patrick, Charles J Cal, Dairen R Jean, and Nicholas F Fell Jr

NOTICES

Disclaimers

The findings in this report are not to be construed as an official Department of the Army position unless so designated by other authorized documents.

Citation of manufacturer's or trade names does not constitute an official endorsement or approval of the use thereof.

Destroy this report when it is no longer needed. Do not return it to the originator.

ARL-TR-8181 ● OCT 2017

US Army Research Laboratory

Detection of Explosives on Surfaces Using UV Raman Spectroscopy: Effect of Substrate Color

by Cole Patrick
University of Oklahoma College of Medicine, Oklahoma City, OK

Charles J Cal
2nd Cavalry Regiment, Camp Vilsek, Germany

Dairen R Jean
1st Cavalry Division, Ft. Hood, TX

Nicholas F Fell Jr
Sensors and Electron Devices Directorate, ARL

REPORT DOCUMENTATION PAGE

Form Approved
OMB No. 0704-0188

1. REPORT DATE *(DD-MM-YYYY)*	2. REPORT TYPE	3. DATES COVERED (From - To)
October 2017	Technical Report	August 2013–June 2016

4. TITLE AND SUBTITLE
Detection of Explosives on Surfaces Using UV Raman Spectroscopy: Effect of Substrate Color

5a. CONTRACT NUMBER

5b. GRANT NUMBER

5c. PROGRAM ELEMENT NUMBER

6. AUTHOR(S)
Cole Patrick, Charles J Cal, Dairen R Jean, and Nicholas F Fell Jr

5d. PROJECT NUMBER

5e. TASK NUMBER

5f. WORK UNIT NUMBER

7. PERFORMING ORGANIZATION NAME(S) AND ADDRESS(ES)
US Army Research Laboratory
Sensors and Electron Devices Directorate (ATTN: RDRL-SEE-E)
2800 Powder Mill Road
Adelphi, MD 20783-1138

8. PERFORMING ORGANIZATION REPORT NUMBER
ARL-TR-8181

9. SPONSORING/MONITORING AGENCY NAME(S) AND ADDRESS(ES)

10. SPONSOR/MONITOR'S ACRONYM(S)

11. SPONSOR/MONITOR'S REPORT NUMBER(S)

12. DISTRIBUTION/AVAILABILITY STATEMENT
Approved for public release; distribution is unlimited.

13. SUPPLEMENTARY NOTES

14. ABSTRACT
Detection of trace levels of explosives on vehicle surfaces is a significant challenge for deployed troops and domestic counterterrorism personnel. The ability to remotely detect a potential vehicle-borne improvised explosive device at a safe distance is a crucial capability. Several companies have proposed UV Raman spectroscopy to meet this need and have constructed and tested systems. One limitation of much of this testing is that it has been performed with bare metal, white-painted, or black-painted surfaces. This investigation seeks to determine the effect of additional colors of vehicle paints with Clearcoat on the ability of UV Raman to detect explosives on these surfaces. The initial results reported here compare visible Raman spectra of Ford Color Standards to the UV Raman spectra of the same panels to determine whether there is any significant background signal in either case. The results clearly show a strong luminescent background in all of the visible Raman spectra and only a weak Raman background signal in the case of UV Raman spectra with 150° backscattering at all 3 UV excitation wavelengths and the onset of luminescence between 1,400 and 1,500 cm^{-1} with 180° backscattering at 257.23-nm excitation.

15. SUBJECT TERMS
UV Raman spectroscopy, explosives, surface characterization, Raman spectroscopy, Raman substrates

16. SECURITY CLASSIFICATION OF:			17. LIMITATION OF ABSTRACT	18. NUMBER OF PAGES	19a. NAME OF RESPONSIBLE PERSON
a. REPORT	b. ABSTRACT	c. THIS PAGE			Nicholas F Fell Jr
Unclassified	Unclassified	Unclassified	UU	28	19b. TELEPHONE NUMBER (Include area code) (301) 394-2560

Contents

List of Figures

List of Tables

Acknowledgments

Funding from the Army Research Office supported this effort.

1. Introduction

The threat of vehicle-borne improvised explosive devices is a pervasive one for deployed US forces and is increasingly a potential threat domestically. A standoff method to identify vehicles carrying these devices or that are part of the supply chain to build such devices is crucial to ensuring the safety of US personnel. UV Raman scattering spectroscopy has been proposed as a candidate technique to meet this need.[1–3]

Numerous other methods have been examined to detect explosives in the environment and on surfaces. Among the techniques used are a group of techniques based on recognition elements immobilized on sensor surfaces that capture and respond to the presence of explosives including antibodies,[4] immunoassays,[5] differential chemical recognition (electronic nose concepts),[6] aptamer-based assays,[7] surface-modified cantilever-based sensors,[8] and surface plasmon resonance sensors.[9] Both traditional mass spectrometry[10] and ion mobility spectrometry[11] have been examined. Optical methods[12] have also been proposed including standoff IR,[13,14] light detection and ranging (LIDAR),[15] laser-induced breakdown spectroscopy (LIBS),[16–19] and photothermal methods.[20] In addition, time-resolved Raman spectroscopy,[21] visible Raman scattering spectroscopy,[22–26] stimulated Raman scattering,[27] surface-enhanced Raman spectroscopy,[28–36] coherent-anti-Stokes Raman spectroscopy,[37] and Raman spectroscopy combined with LIBS[38–40] have been investigated. UV Raman spectroscopy[41–57] has also been demonstrated both alone and in combination with LIBS.[40,58–62]

UV Raman provides several advantages over other methods.[63] When UV Raman is used below 300 nm, it takes advantage of the "solar blind" region where sunlight is absorbed by the ozone layer and little background is observed. In addition, the potential fluorescence background that frequently plagues Raman spectroscopy is reduced by excitation below 250 nm, by either not being excited or being shifted to sufficiently high wavelengths such that the Raman signal is background-free. While UV light is more strongly absorbed by the atmosphere, standoff ranges in the tens of meters have been reported.

The testing of UV Raman spectroscopy systems for standoff UV Raman spectroscopy has been generally limited to bare metal, white, black, and a small number of colored targets.[58–62] To fully test the capability of UV Raman spectroscopy to detect explosive traces on surfaces, it will be necessary to test substrates with additional colors. The goal of this project is to determine whether colored substrates will interfere with the ability of UV Raman spectroscopy to

detect traces of explosives on surfaces. This report describes our initial results examining over a dozen Ford standard panels for their background signals in the visible and UV.

2. Experiment

2.1 Materials

The color panels used were Ford Color Standards (ACT Test Panels). Fourteen different colors were chosen for these tests based on the number of models of vehicles using them and the frequency with which they are observed on the roads. Table 1 lists the colors and their M-code numbers. The panels were used as received. Examples of the panels are shown in Fig. 1. The following chemicals were obtained from Sigma Aldrich and were used as received, without further purification: 2,4-dinitrotoluene (2,4-DNT), 2,6-dinitrotoluene (2,6-DNT), acetonitrile, and tetrahydrofuran.

Table 1 Ford standard panels used in experiments

Standard	M-code
School Bus Yellow	M6284
Vermillion Red	M6470
Pueblo Gold	M7113
Sterling Gray Metallic	M7205
Ingot Silver Metallic	M7226
Ginger Ale	M7262
Green Gem	M7289
Oxford White	M6466
Dark Pearl Blue	M7083
White Titanium Tricoat	M7204
Tuxedo Black Metallic	M7211
Kodiak Brown	M7261
Ruby Red	M7283
Deep Impact Blue	M7296

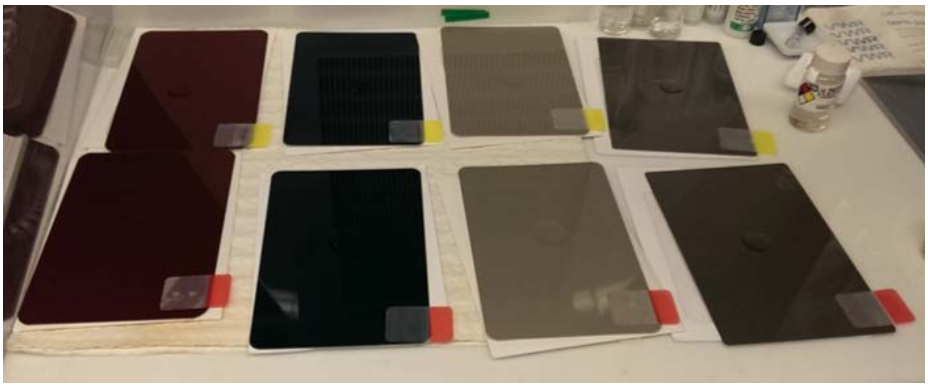

Fig. 1 Examples of Ford standard panels being dried after deposition of 2,4-DNT and 2,6-DNT from acetonitrile slurry

2.2 Instrumentation

IR spectra were collected on a Jasco FT/IR-4100 (Easton, MD) with a Jasco ATR-PRO450-S diamond single-pass attenuated total reflection (ATR) assembly (Easton, MD). Spectra were collected with 4 cm^{-1} resolution and 64 accumulations. Two different Raman systems were utilized in these experiments. The visible Raman system used a Lexel 95L argon (Ar) ion laser (Cambridge Lasers Laboratories, Fremont, CA) at 488 nm with an Acton SP2500A 500-mm focal length monochromator and a PIXIS 400 × 3048 pixel charge-coupled device (CCD) camera (Princeton Instruments, Trenton, NJ). An InPhotonics 488-nm RamanProbe Raman fiber-optic assembly (InPhotonics, Norwood, MA) was used to deliver the excitation and collect the Raman scattered light. The fiber probe contains filters to remove the Rayleigh scattered light before it enters the emission fiber. Spectra were collected with 90-mW of excitation power at the laser head, 1-s integration time, and 100 accumulations. Figure 2 shows the optical arrangement for this system.

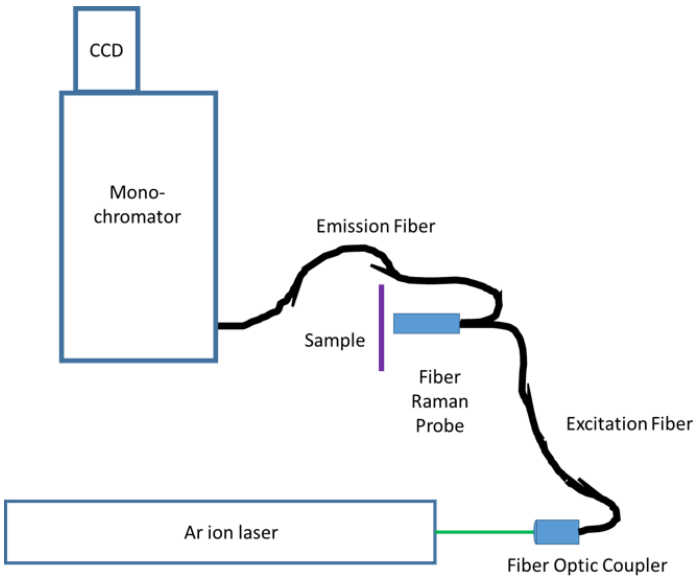

Fig. 2 Visible Raman optical train

The UV Raman spectra were collected using a Lexel 95-SHG frequency doubled Ar ion laser (Cambridge Lasers Laboratories, Fremont, CA) with an Acton TriVista 555 triple monochromator (Princeton Instruments, Trenton, NJ) and a PIXIS 2KBUV, 2048 × 512 pixel, UV-enhanced, backthinned CCD camera (Princeton Instruments, Trenton, NJ). The TriVista triple monochromator was equipped with UV-enhanced gratings with 1,800 grooves/mm in the first 2 monochromators, which comprise the filter stage, and 3,600 grooves/mm in the third monochromator, which serves as the spectrograph stage. Spectra were collected with 1- to 5-s integration times, depending on the signal level, and 100 accumulations. Spectra were collected of the blank panels at 229-, 244-, and 257.23-nm excitation wavelengths by changing the doubling crystal in the laser to change the excitation wavelength. The power of the laser was also varied with spectra collected at 1-, 5-, 10-, and 25-mW excitation power, when the power level desired was available. The initial background study was performed with the collection optics in a 150° backscatter arrangement. Figure 3 shows the optical arrangement of this system.

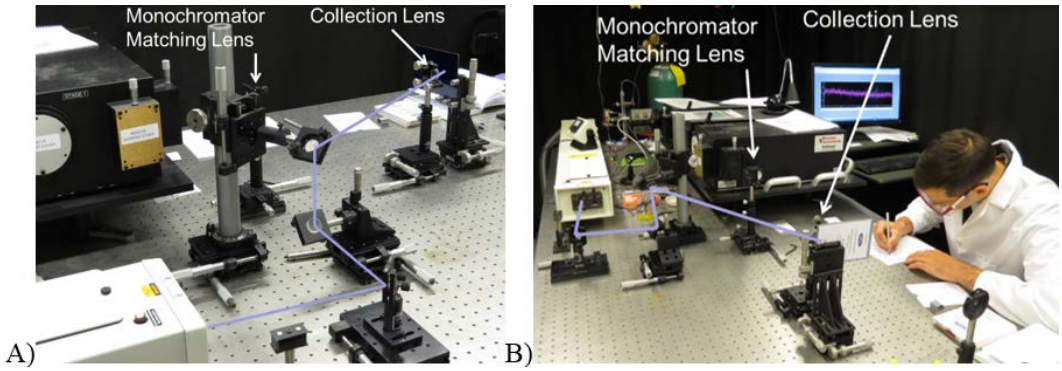

Fig. 3 Optical train for 150° backscattering arrangement. A) The frequency doubled Ar-ion laser is located in the lower left corner of the image. The triple monochromator is located in the upper left corner of the image. B) The frequency doubled Ar-ion laser is located in the upper left corner of the image. The Princeton Instruments TriVista triple monochromator is located in the center of the image.

Later work was performed using an off-axis parabolic mirror (MPD249HF01SP, Thor Labs, Newton, NJ) to collect Raman scattering at 180°. The move to 180° backscattering was precipitated by difficulty obtaining UV Raman spectra from solid samples. It was also determined that the height adjustment needed to be separated from changing the beam path to preserve the vertical polarization of the excitation beam. The TriVista system UV-enhanced gratings have a highly polarization-dependent response, so it was necessary to ensure that the excitation and collected Raman photons had the vertical polarization to match the highest throughput of the monochromator system. Figure 4 shows this optical arrangement.

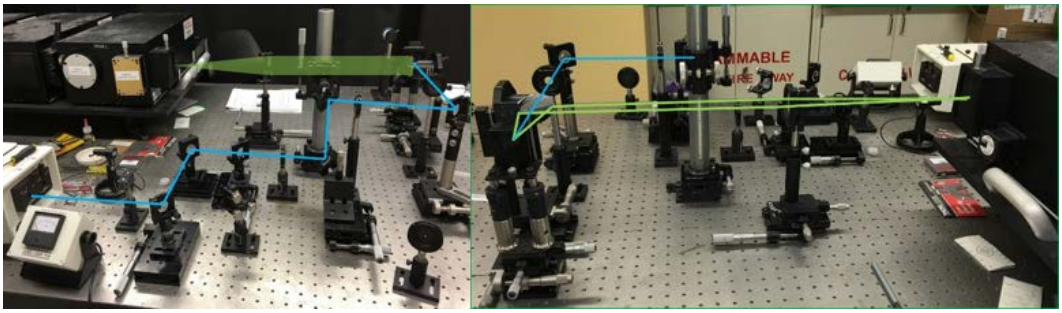

Fig. 4 Optical arrangement for UV Raman 180° backscattering measurements. Blue line indicates laser excitation path and green indicates Raman scattering.

3. Results and Discussion

IR absorption spectra are frequently used for forensic examination of car paint and identification of vehicles involved in criminal activities.[64–65] The spectra of the Ford standard panels are shown in Figs. 5 and 6. Figure 5 shows the entire spectra collected using Fourier-transform IR spectroscopy (FTIR)-ATR absorption, and

Fig. 6 shows more focused spectra on the nitrile and C-H and O-H stretching regions. Clearly visible differences are evident among the panels based on differences in the pigments used and potentially on the Clearcoat used as well. The literature in this area is focused on the use of the spectra rather than their interpretation, so further investigation is necessary to discuss them more completely. It is clear from visual examination of the spectra that they all contain nitrile bands in the 2,300–2,400 cm^{-1} region. This is perhaps indicative of an acrylonitrile polymer as part of the Clearcoat. The fingerprint region indicates a mixture of polymer and pigment bands. This region will be further investigated.

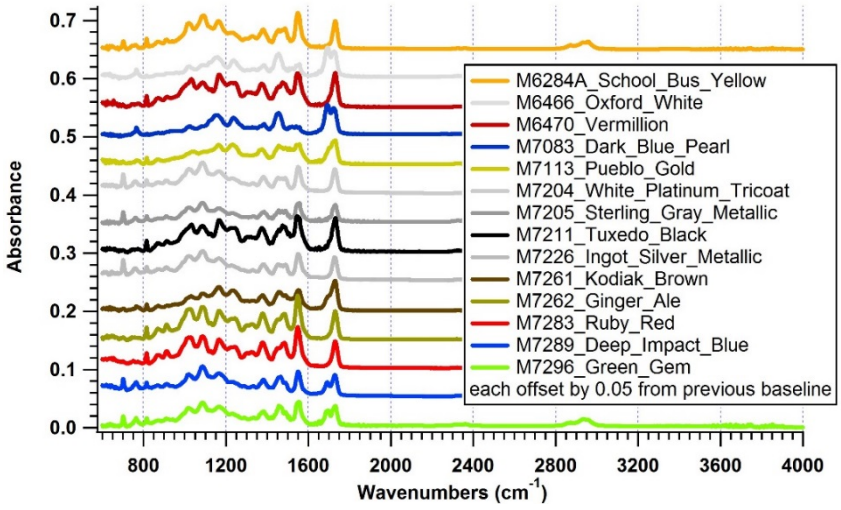

Fig. 5 FTIR-ATR absorption spectra for Ford standard panels. Each spectrum is offset 0.05 absorbance units from the one below it.

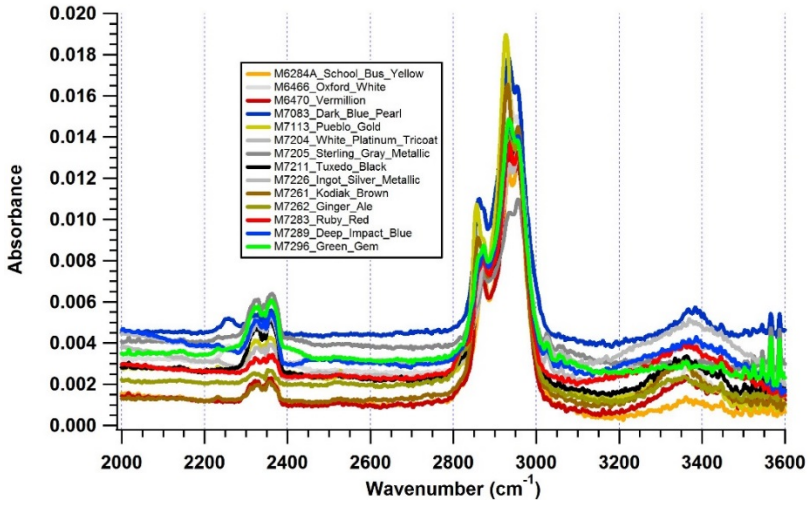

Fig. 6 FTIR-ATR absorption spectra of Ford standard panels highlighting the nitrile and C-H and O-H stretching regions that were obscured in Fig. 5

Collecting spectra using visible wavelength excitation poses significant challenges with the various colored panels. Both a strong luminescence and highly variable response were observed as shown in Figs. 7 and 8. When operating with visible wavelength excitation (488 nm), each panel had significantly different background spectra. More specifically, there was a trend toward lighter color panels exhibiting stronger luminescence backgrounds. The cause of the differing background spectra is most likely due to varying levels of fluorescent components in the pigments and Clearcoat. Consequently, because of the higher background activity in the visible spectra, any hopes of being able to distinguish any sort of Raman peaks are lost.

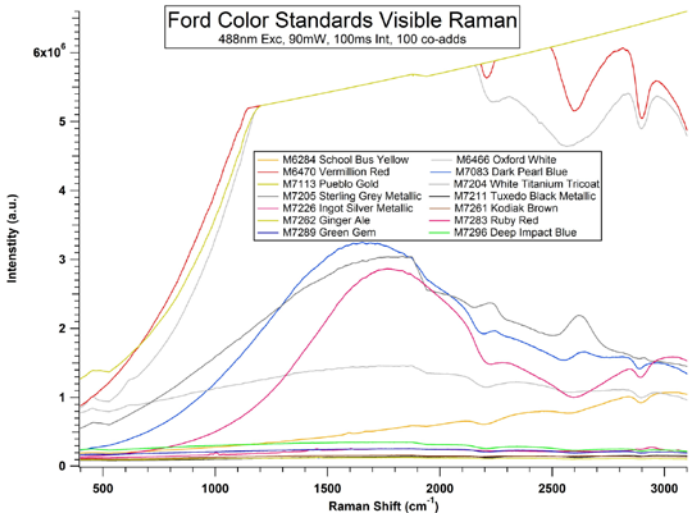

Fig. 7 Visible Raman spectra of Ford standard panels. Excitation was at 488 nm (90 mW at the laser) with a 100-ms integration time and 100 accumulations. The samples were excited and the Raman scattering collected with a 488-nm InPhotonics Raman probe fiber-optic assembly.

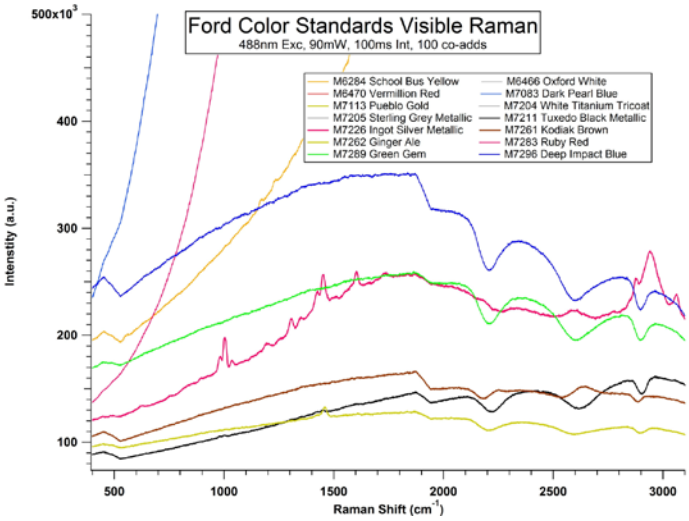

Fig. 8 Visible Raman spectra of Ford standard panels. Rescaling of Fig. 7 to highlight the weaker luminescence observed with some of the panels. Excitation was at 488 nm (90 mW at the laser) with a 100-ms integration time and 100 accumulations. The samples were excited and the Raman scattering collected with a 488-nm InPhotonics Raman Probe fiber-optic assembly.

UV excitation provides much more useful background spectra that should be useful in the future detection of explosives. Figure 9 shows the background spectra of every color standard tested using the 150° backscattering geometry (Fig. 3), each one being offset slightly to show comparison rather than overlap of the spectra. With UV excitation, the background spectra did not differ significantly between different colored panels. Furthermore, there were no noticeable differences in background spectra when using different UV wavelengths or laser powers. Figure 10 compares the spectra from one panel being tested using the 3 UV wavelengths with one using a visible wavelength. One of the limitations observed with this geometry is that the polarization of the collected Raman scattering only partially matches the preferred polarization of the monochromator gratings. Therefore, it is unclear whether the low background signal is due to the small amount of light reaching the detector or a low background signal. We were unable to collect Raman spectra of solid samples in this geometry and only saw weak spectra from liquid samples. For these reasons, we switched to the 180° backscattering geometry (Fig. 4).

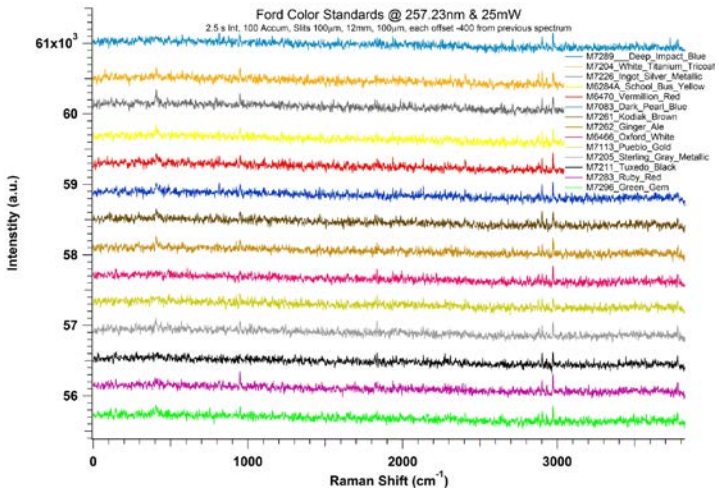

Fig. 9 UV Raman scattering collected at the 150° backscattering geometry (Fig. 3) for Ford standard panels. Spectra were collected with 257.23-nm excitation (25 mW at the laser) using 2.5-s integration time and 100 accumulations. Each spectrum is offset by 400 counts from the one below it.

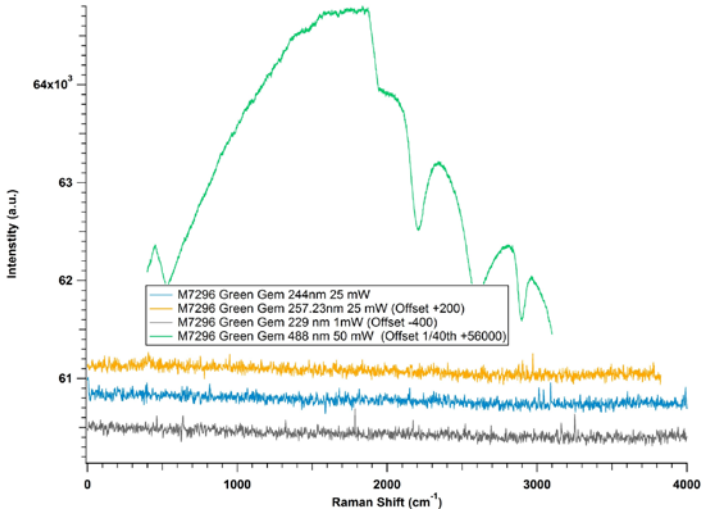

Fig. 10 Comparison of Raman scattering from 3 UV wavelengths (229, 244, and 257.23 nm) with 488 nm for one of the Ford standard panels (M7296 Green Gem). The UV Raman spectra were offset by 200 counts from the one below them. The 488-nm Raman spectrum was divided by 40 and then offset by 56,000 to be on-scale with the UV Raman spectra. All UV Raman spectra were collected with the 150° backscattering geometry with 2.5-s integration times and 100 accumulations.

In the 180° backscattering geometry (Fig. 4), signals were observed from both liquid and solid samples. Figure 11 depicts the background Raman scattering and luminescence onset from excitation at 257.23 nm. In addition to the change in excitation and collection geometry, a new set of gratings was obtained for the system that is better optimized for the UV. These grating have twice the groove

density, so one-half of the spectral range collected previously can be observed without moving the gratings in this case. As can be seen in these spectra, several colors exhibited a luminescence background beginning as a Raman shift between 1,400 and 1,500 cm^{-1}. As with the visible Raman results (Fig. 7), the luminescence tends to be stronger for lighter and brighter panel colors. These results suggest that excitation at 257.23 nm may not be suitable for detection of trace explosives on all possible colors of vehicles. We will continue to investigate the use of 257.23 nm, but will also shift to 244 and 229 nm to determine whether the background at those wavelengths is more suitable for surface contamination determinations. The colors with the strongest luminescence background are the White Titanium Tricoat, Sterling Gray Metallic, Ingot Silver Metallic, Green Gem, and Deep Impact Blue panels. The School Bus Yellow, Oxford White, Dark Pearl Blue, and Kodiak Brown panels showed lower but clearly observable luminescence backgrounds. The similarity may lie more in the Clearcoat composition rather than the pigments. Further investigation will be required to determine the best excitation wavelength for the detection of surface explosive traces.

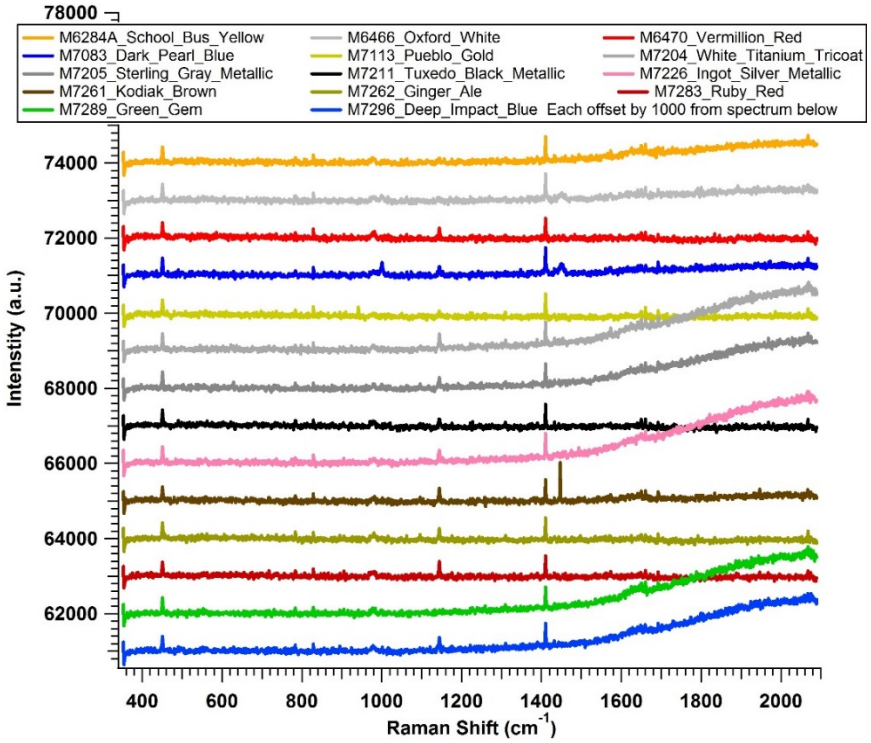

Fig. 11 UV Raman scattering collected at the 180° backscattering geometry (Fig. 4) for Ford standard panels. Spectra were collected with 257.23-nm excitation (10 mW at the laser) using 1.0-s integration time and 100 accumulations. Each spectrum is offset by 1,000 counts from the one below it.

4. Future Work

Several aspects of the project remain to be investigated during the remainder of the academic year 2016. First, efforts will be made to interpret the fingerprint region of the IR spectra of the blank panels to better understand the chemical nature of pigments and Clearcoat. We will also investigate the background of the blank panels in the other 2 UV excitation wavelengths (244 and 229 nm) we have available. Finally, we will continue to pursue determinations of the limits of detection of explosives in the Ford standard panels. This will entail both evaporative deposition from tetrahydrofuran solutions and more control depositions provided by US Army Research Laboratory scientists using their inkjet printing method.[66]

5. Conclusions

After determining that the visible spectrum does not effectively permit elucidation of the DNT peaks, the UV spectrum was found to be a better approach to the solution because it results in minimal background scattering. The color of the panel, wavelength of the UV laser, and the power of the laser do not significantly affect the background spectra while in the UV spectrum in 150° backscattering. Therefore, UV wavelengths should be used in explosive detection because of the minimal and consistent background scattering across all panels of different colors. However, in 180° backscattering, where the monochromator grating polarizations are better matched, some luminescence was observed under UV excitation. Future experiments will be conducted to determine the optimum excitation wavelength and the limits of detection of surface explosive traces for our system. Consequently, explosive detection using UV wavelengths should provide for a consistent measurement without the complications found when using visible excitation.

6. References

1. Nagli L, Gaft M. Raman scattering spectroscopy for explosives identification. In: Wood GL, Dubinskii MA, editors. Proc. SPIE. 6552, Laser Source Technology for Defense and Security III; 2007 May 15; Orlando, FL. Bellingham (WA): Society of Photo-Optical Instrumentation Engineers; c2007. p. 65520Z. doi: 10.1117/12.719319.

2. Tuschel DD, Mikhonin AV, Lemoff BE, Asher AS. Deep ultraviolet resonance Raman Excitation enables explosives detection. Appl Spectrosc. 2010;64(4):425–432.

3. Ford AR, McVay T, Waterbury R, Vunck D, Rose J, Blank T, Pohl K, Dottery E, Hankus M, Holthoff E, et al. Explosives sensing using multiple optical techniques in a standoff regime with a common platform. Defense and Homeland Security. April 2011;6–11. www.spectroscopyonline.com.

4. Altstein M, Bronshtein A, Glattstein B, Zeichner A, Tamirir T, Almog J. Immunochemical approaches for purification and detection of TNT traces by antibodies entrapped in a sol-gel matrix. Anal Chem. 2001;73:2461–2467.

5. Wilson R, Clavering C, Hutchinson A. Electrochemiluminescence enzyme immunoassays for TNT and pentaerythritol tetranitrate. Anal Chem. 2003;75:2004–2011.

6. Andrew TL, Swager TM. A fluorescence turn-on mechanism to detect high explosives RDX and PETN. J Am Chem Soc. 2007;129:7254–7255.

7. Ho MY, D'Souza N, Migliorato P. Electrochemical aptamer-based sandwich assays for the detection of explosives. Anal Chem. 2012;84:4245–4247.

8. Lee D, Kim S, Jeon S, Thundat T. Direct detection and speciation of trace explosives using a nanoporous multifunctional microcantilever. Anal Chem. 2014;86:5077–5082.

9. Bharadwaj R, Mukherji S. Gold nanoparticle coated U-bend fiber optic probe for localized surface plasmon resonance based detection of explosive vapours. Sensors and Actuators B. 2014;192:804–811.

10. Mullen C, Irwin A, Pond BV, Huestis DL, Coggiola MJ, Oser H. Detection of explosives and explosives-related compounds by single photon laser ionization time-of-flight mass spectrometry. Anal Chem. 2006;78:3807–3814.

11. Zalewska A, Pawlowski W, Tomaszewski W. Limits of detection of explosives as determined with IMS and field asymmetric IMS vapour detectors. Forensic Science International. 2013;226:168–172.

12. Pellegrino PM, Holthoff EL, Farrell ME, editors. Laser-based optical detection of explosives. Boca Raton (FL): CRC Press; 2015.

13. Hernandez-Riveria SP, Castro-Suarez JR, Pacheo-Londono LC, Rey-Villamizar N, Velez-Reyes M, Diem M. Mid-infrared vibrational spectroscopy standoff detection of highly energetic materials: new developments. Defense and Homeland Security. April 2011;34–41. www.spectroscopyonline.com.

14. Fuchs F, Hugger S, Kinzer M, Yang QK, Bronner W, Aidam R, Degreif K, Rademacher S, Schnurer F, Schweikert W. Standoff detection of explosives with broad band tunable external cavity quantum cascade lasers. In: Razeghi M, Tournie E, Brown GJ, editors. Proc. SPIE 8268, Quantum Sensing and Nanophotonic Devices IX; 2012 Jan 21; San Francisco, CA. Bellingham (WA): Society of Photo-Optical Instrumentation Engineers; c2012. p. 82681N.

15. Forest R, Babin, F, Gay D, Ho N, Pancrati O, Deblois S, Desilets S, Maheux J. Use of spectroscopic lidar for standoff explosives detection through Raman spectra. In: Fountain AW 3rd, editor. Proc. SPIE 8358, Chemical, Biological, Radiological, Nuclear, and Explosives (CBRNE) Sensing XIII; 2012 May 5; Baltimore, MD. Bellingham (WA): Society of Photo-Optical Instrumentation Engineers; c2012. p. 83580M.

16. Cremers DA, Chinni RC. Laser-induced breakdown spectroscopy–capabilities and limitations. Appl Spectroscopy Rev. 2009;44(6):457–506.

17. De Lucia FC, Gottfried JL. Influence of molecular structure on the laser-induced plasma emission of the explosive RDX and organic polymers. J Phys Chem A. 2013;117:9555–9563.

18. Brady JJ, Roberson SD, Farrell ME, Holthoff EL, Stratis-Cullum DN, Pellegrino PM. Laser-induced breakdown spectroscopy: a review of applied explosive detection. Adelphi (MD): Army Research Laboratory (US); 2013. Report No.: ARL-TR-6649.

19. Gaona I, Serrano J, Moros J, Laserna JJ. Range-adaptive standoff recognition of explosive fingerprints on solid surfaces using a supervised learning method and laser-induced breakdown spectroscopy. Anal Chem. 2014;86:5045–5052.

20. Kendziora CA, Furstenberg R, Papantonakis MR, Nguyen VK, Byers JM, McGill RA. Photothermal methods for laser-based detection of explosives. In:

Pellegrino PM, Holthoff EL, Farrell ME, editors. Laser-based optical detection of explosives. Boca Raton (FL): CRC Press; 2015. p. 257–288.

21. Petterson IEI, Lopez-Lopez M, Garcia-Ruiz C, Gooijer C, Buijis JB, Ariese F. Noninvasive detection of concealed explosives: depth profiling through opaque plastics by time-resolved Raman spectroscopy. Anal Chem. 2011;83:8517–8523.

22. Östmark H, Nordberg M, Carlsson TE. Stand-off detection of explosives particles by multispectral imaging Raman spectroscopy. Appl Optics. 2011;50(28):5592–5599.

23. Misra AK, Sharma SK, Acosta TE, Porter JN, Bates DE. Single-pulse standoff Raman detection of chemicals from 120 m distance during daytime. Appl Spectrosc. 2012;66(11):1279–1285.

24. Kanchanapally R, Sinha SS, Fan Z, Dubey M, Zakar E, Ray PC. Graphene oxide-gold nanocage hybrid platform for trace level identification of nitro explosives using Raman fingerprint. J Phys Chem C. 2014;118:7070–7075.

25. Bueno J, Sikirzhytski V, Lednev IK. Raman spectroscopic analysis of gunshot residue offering great potential for caliber differentiation. Anal Chem. 2012;84;4334–4339.

26. Carter JC, Angel SM, Lawrence-Snyder M, Scaffidi J, Whipple RE, Reynolds JG. Standoff detection of high explosives materials at 50 meters in ambient light conditions using a small Raman instrument. Appl Spectrosc. 2005;59(6):769–775.

27. Bremer MT, Dantus M. Standoff explosives trace detection and imaging by selective stimulated Raman scattering. Appl Phys Lett. 2013;102:06119. doi:10.1063/1.4817248.

28. Muehlethaler C, Leona M, Lombardi JR. Review of surface enhanced Raman scattering applications in forensic science. Anal Chem. 2016;88:152–169.

29. Sylvia JM, Janni JA, Klein JD, Spencer KM. Surface-enhanced Raman detection of 2,4-dinitrotoluene impurity vapors as a marker to locate landmines. Anal Chem. 2000;72:5834–5840.

30. Botti S, Almaviva S, Cantarini L, Palucci A, Puiu A, Rufoloni A. Trace level detection and identification of nitro-based explosives by surface-enhanced Raman spectroscopy. J Raman Spectrosc. 2013;44:463–468.

31. Xu Z, Hao J, Braida W, Strickland D, Li F, Meng X. Surface-enhanced Raman scattering spectroscopy of explosive 2,4-dinitroanisole using modified silver nanoparticles. Langmuir. 2011;27:13773–13779.

32. Sil S, Chaturvedi D, Krishnappa KB, Kumar S, Asthana SN, Umapathy S. Density functional theoretical modeling, electrostatic surface potential and surface enhanced Raman spectroscopic studies on biosynthesized silver nanoparticles: observation of 400 pM sensitivity to explosives. J Phys Chem A. 2014;118:2904–2914.

33. Jamil AKM, Izake EL, Sivanesan A, Fredericks PM. Rapid detection of TNT in aqueous media by selective label free surface enhanced Raman spectroscopy. Talanta. 2015;134:732–738.

34. Tian L, Nergiz SZ, Farrell ME, Pellegrino PM, Slocik JM, Naik RR, Singamaneni S. Plasmonic paper for trace detection of analytes. SPIE Newsroom. 2014 June 2. doi: 10.1117/2.1201405.005468.

35. Piorek BD, Lee SJ, Moskovits M, Meinhart CD. Free-surface microfluidics/surface-enhanced Raman spectroscopy for real-time trace vapor detection of explosives. Anal Chem. 2012;84:9700–9705.

36. Wang J, Yang L, Liu B, Jiang H, Liu R, Yang J, Han G, Mei Q, Zhang Z. Inkjet-printed silver nanoparticle paper detects airborne species from crystalline explosives and their ultratrace residues in open environment. Anal Chem. 2014;86:3338–3345.

37. Dogariu A, Pidwerbetsky A. Coherent anti-Stokes Raman spectroscopy for detecting explosives in real-time. In: Fountain AW 3rd, editor. Proc. SPIE 8358, Chemical, Biological, Radiological, Nuclear, and Explosives (CBRNE) Sensing XIII; 2012 May 5; Baltimore, MD. Bellingham (WA): Society of Photo-Optical Instrumentation Engineers; c2012. p. 83580R.

38. Moros J, Lorenzo JA, Lucena P, Tobaria LM, Laserna JJ. Simultaneous Raman spectroscopy-laser-induced breakdown spectroscopy for instant standoff analysis of explosives using a mobile integrated platform. Anal Chem. 2010;82:1389–1400.

39. Moros J, Laserna JJ. New Raman-laser-induced breakdown spectroscopy identity of explosives using parametric data fusion on an integrated sensing platform. Anal Chem. 2011;83:6275–6285.

40. Lin Q, Niu G, Wang Q, Yu Q, Duan Y. Combined laser-induced breakdown with Raman spectroscopy: historical technology development and recent applications. Appl Spectroscopy Reviews. 2013;48:487–508.

41. Lacey RJ, Hayward IP, Sands HS, Batchelder DN. Characterization and identification of contraband using UV resonant Raman spectroscopy. Proc. SPIE 2937, Enabling Technologies for Law Enforcement and Security; 1996; Boston, MA. Bellingham (WA): Society of Photo-Optical Instrumentation Engineers; c1997. p. 100–105.

42. Wu M, Ray M, Fung KH, Ruckman MW, Harder D, Sedlacek AJ 3rd. Stand-off detection of chemicals by UV Raman spectroscopy. Appl Spectrosc. 2000;54(6):800–806.

43. Tuschel DD, Mikhonin AV, Lemoff BE, Asher SA. Deep ultraviolet resonance Raman excitation enables explosives detection. Appl Spectrosc. 2010;64(4):425–432.

44. Ghosh M, Wang L, Asher SA. Deep-ultraviolet resonance Raman excitation profiles of NH_4NO_3, PETN, TNT, HMX, and RDX. Appl Spectrosc. 2012;66(9):1013–1021.

45. Comanescu G, Manka CK, Grun J, Nikitin S, Zabetakis D. Identification of explosives with two-dimensional ultraviolet resonance Raman spectroscopy. Appl Spectrosc. 2008;62(8):833–839.

46. Emmons ED, Tripathi A, Guicheteau JA, Fountain AW 3rd, Christesen SD. Ultraviolet resonance Raman spectroscopy of explosives in solution and the solid state. J Phys Chem A. 2013;117:4158–4166.

47. Gaft M, Nagli L. UV gated Raman spectroscopy for standoff detection of explosives. Optical Materials. 2008;30:1739–1746.

48. Nagli L, Gaft M, Fleger Y, Rosenbluh M. Absolute Raman cross-sections of some explosives: trends to UV. Optical Materials. 2008;30:1747–1754.

49. Ballesteros LM, Herrara GM, Castro ME, Briano J, Mina N, Hernandez-Rivera SP. Spectroscopic signatures of PETN in contact with sand particles. In: Harmon RS, Broach JT, Holloway JH Jr, editors. Proc. SPIE 5794; Detection and Remediation Technologies for Mines and Minelike Targets X; 2005; Orlando, FL. Bellingham (WA): Society of Photo-Optical Instrumentation Engineers; c2005. p. 1254–1262.

50. Blanco A, Pacheco-Londono LC, Pena-Quevedo AJ, Hernandez-Rivera SJ. UV Raman detection of 2,4-DNT in contact with sand particles. In: Harmon RS, Broach JT, Holloway JH Jr, editors. Proc. SPIE 6217; Detection and Remediation Technologies for Mines and Minelike Targets XI; 2006; Orlando, FL. Bellingham (WA): Society of Photo-Optical Instrumentation Engineers; c2006. p. 621737.

51. Al-Saidi WA, Asher SA, Norman P. Resonance Raman spectra of TNT and RDX using vibronic theory, excited-state gradient, and complex polarizability approximations. J Phys Chem A. 2012;116:7862–7872.

52. Skvortsov LA. Laser methods for detecting explosive residues on surfaces of distant objects. Quantum Electronics. 2012;42(1):1–11.

53. Almaviva S, Angelini F, Chirico R, Palucci A, Nuvoli M, Schnuerer F, Schweikert W, Romolo FS. Eye-safe UV Raman spectroscopy for remote detection of explosives and their precursors in fingerprint concentrations. In: Burgess D, Zamboni R, et al., editors. Proc. SPIE 9253; Optics and Photonics for Counterterrorism, Crime Fighting, and Defense X; and Optical Materials and Biomaterials in Security and Defense Systems Technology XI; 2014; Amsterdam, Netherlands. Bellingham (WA): Society of Photo-Optical Instrumentation Engineers; c2014. p. 925303.

54. Fleger Y, Nagli L, Gaft M, Rosenbluh M. Narrow gated Raman and luminescence of explosives. J Luminescence. 2009;129:979–983.

55. Yellampalle B, Sluch M, Wu H-S, Martin R, McCormick W, Ice R, Lemoff BE. Dual-excitation-wavelength resonance-Raman explosives detector. In: Fountain AW, Editor. Proc. SPIE 8710; Chemical, Biological, Radiological, Nuclear, and Explosives (CBRNE) Sensing XIV; 2013; Baltimore, MD. Bellingham (WA): Society of Photo-Optical Instrumentation Engineers; c2013. p. 87100Z.

56. Chirico R, Almaviva S, Botti S, Cantarini L, Colao F, Fiorani L, Nuvoli M, Palucci A. Stand-off detection of traces of explosives and precursors on fabrics by UV Raman spectroscopy. In: Lewis C, Burgess D, editors. Proc. SPIE 8546, Optics and Photonics for Counterterrorism, Crime Fighting, and Defence VIII; 2012; Edinburgh, UK. Bellingham (WA): Society of Photo-Optical Instrumentation Engineers; c2102. p. 85460W.

57. Ehlerding A, Johansson I, Wallin S, Östmark H. Resonance-enhanced Raman spectroscopy on explosives vapor at standoff distances. Intl J of Spectros. 2012;2012. Article ID 158715.

58. Waterbury RD, Pal A, Killinger DK, Rose J, Dottery EL, Ontai G. Standoff LIBS measurements of energetic materials using a 266 nm excitation laser. In: Fountain AW 3rd, Gardner PJ, editors. Proc. SPIE 6954, Chemical, Biological, Radiological, Nuclear, and Explosives (CBRNE) Sensing IX; Orlando, FL. Bellingham (WA): Society of Photo-Optical Instrumentation Engineers; c2008. p. 695409.

59. Waterbury RD, Ford AR, Rose JB, Dottery EL. Results of a UV TEPS-Raman energetic detection system (TREDS-2) for standoff detection. In: Fountain AW 3rd, Gardner PJ, editors. Proc. SPIE 7304, Chemical, Biological, Radiological, Nuclear, and Explosives (CBRNE) Sensing X; 2009; Orlando, FL. Bellingham (WA): Society of Photo-Optical Instrumentation Engineers; c2009. p. 73041B.

60. Ford A, Waterbury RD, Rose J, Dottery EL. Standoff detection of hazardous materials using a novel dual laser pulse technique: theory and experiments. In: Fountain AW 3rd, Gardner PJ, editors. Proc. SPIE 7304, Chemical, Biological, Radiological, Nuclear, and Explosives (CBRNE) Sensing X; 2009; Orlando, FL. Bellingham (WA): Society of Photo-Optical Instrumentation Engineers; c2009. p. 73041C.

61. Waterbury R, Rose J, Vunck D, Blank T, Pohl K, Ford A, McVay T, Dottery E. Fabrication and testing of a standoff trace explosives detection system. In: Fountain AW 3rd, Gardner PJ, editors. Proc. SPIE 8018, Chemical, Biological, Radiological, Nuclear, and Explosives (CBRNE) Sensing XII; 2011; Orlando, FL. Bellingham (WA): Society of Photo-Optical Instrumentation Engineers; c2011. p. 801818.

62. Waterbury R, Vunck D, Hopkins AJ, Pohl K, Ford A, Dottery E. Recent improvements and testing of a check point explosives detection system. In: Fountain AW 3rd, editor. Chemical, Biological, Radiological, Nuclear, and Explosives (CBRNE) Sensing XIII, Proc. of SPIE, 2012; vol. 8358; p. 83580N.

63. Izake EL. Forensic and homeland security applications of modern portable Raman spectroscopy. Forensic Science International. 2010;202:1–8.

64. Zieba-Palus J, Michalska A, Weselucha-Birczynska A. Characterisation of paint samples by infrared and Raman spectroscopy for criminalistics purposes. J Molecular Structure. 2011;993:134–141.

65. Zieba-Palus J, Borusiewicz R. Examination of multilayer paint coats by the use of infrared, Raman, and XRF spectroscopy for forensic purposes. J Molecular Structure. 2006;792–793:286–292.

66. Emmons ED, Farrell ME, Holthoff EL, Tripathi A, Green N, Moon RP, Guicheteau JA, Christesen SD, Pellegrino PM, Fountain AW 3rd. Characterization of polymorphic states in energetic samples of 1,3,5-trinitro-1,3,5-triazine (RDX) fabricated using drop-on-demand inkjet technology. Appl Spectrosc. 2012;66(6):628–635.

List of Symbols, Abbreviations, and Acronyms

2,4-DNT	2,4-dinitrotoluene
2,6-DNT	2,6-dinitrotoluene
Ar	argon
ATR	attenuated total reflection
CCD	charge-coupled device
FTIR	Fourier-transform infrared spectroscopy
IR	infrared
LIBS	laser-induced breakdown spectroscopy
LIDAR	light detection and ranging
UV	ultraviolet

1 (PDF) DEFENSE TECHNICAL INFORMATION CTR DTIC OCA

2 (PDF) DIR ARL
RDRL DCM
IMAL HRA RECORDS MGMT
RDRL IRB
TECH LIB

1 (PDF) GOVT PRINTG OFC
A MALHOTRA

1 (PDF) NAVAL SURFACE WARFARE CTR
EOD TECHDIV
M SHEPARD

1 (PDF) DEPT OF HOMELAND SECURITY
HSARPA
R BENJAMIN

1 (PDF) USMA
MADN-PRC
K INGOLD

5 (PDF) DIR ARL
RDRL SEE
G WOOD
RDRL SEE E
N FELL JR
P PELLEGRINO
E HOLTHOFF
M FARRELL